Rectangular Thermal Doublers of Uniform Thickness

R. P. Bobco* and R. P. Starkovs†
Hughes Aircraft Company, Los Angeles, California

An infinite series solution is developed for the steady temperature field in a thin, rectangular region exposed to a piecewise continuous heat flux and losing energy from exposed surfaces either by linearized radiation or true convection. The geometry and environmental conditions approximate a spacecraft application in which a fin-like plate (thermal doubler) is used to enhance the radiating area of an energy-dissipating electronic component mounted in an equipment bay. A numerical example, based on typical spacecraft power and environmental conditions, is used to show how the closed-form solution may be used to investigate geometrical influences. Both direct (i.e., specified thickness, unknown temperature) and design (i.e., specified temperature, unknown thickness) problems are examined to show how temperature and doubler thickness depend on the shape of the heated area ("footprint"), the shape of the doubler, and the location of the footprint within the doubler boundaries. The numerical results indicate that the two-dimensional solution for a case with double symmetry is bounded by the one-dimensional solutions for a circular footprint/circular doubler and a simple Cartesian geometry. The present formulation will be useful both for the trade studies leading to a preliminary design and as an exact solution for calibrating nodal models.

Nomenclature

A = area, m^2
Bi = Biot modulus, $h\ell_3/k$
b = thickness parameter, $(Bi\ell_3/\delta_0)^{1/2}$
C_{jn} = constant of integration
$\mathcal{F}$ = radiation interchange factor
h = surface heat loss coefficient, W/m^2-K
k = thermal conductivity, W/m-K
ℓ = length in x direction, m
L = nondimensional length, ℓ/ℓ_3
q = heat flux, W/m^2
T = temperature, °C or K
U = overall heat-transfer coefficient, W/m^2-K
w = width in y direction, m
W = nondimensional width, w/ℓ_3
x,y = Cartesian coordinates, m
δ_0 = doubler thickness, m
ζ = eigenvalue, Eq. (13)
η = nondimensional coordinate, y/ℓ_3
λ = doubler or footprint shape parameter, Eqs. (15a) and (15b)
ν = footprint location parameter, Eq. (15c)
ξ = nondimensional coordinate, x/ℓ_3
σ = Stefan-Boltzmann constant, W/m^2-K^4
ϕ = nondimensional temperature, $[T(\xi,\eta)-T_\infty]/(q_0\ell_3/k)$

Introduction

PASSIVE techniques are commonly used to control the temperatures of electronic components employed in unmanned spacecraft. Electronic equipment is usually mounted on a shelf enclosed by spacecraft surfaces which include solar panels, radiators, and multilayer insulation blankets. Traveling wave tubes and many other temperature-sensitive electronic components have inadequate surface areas to allow direct energy transport to heat sink regions; in such instances, power-dissipating components are mounted to lightweight metal sheets with high thermal conductivity to enhance the surface area for energy transport. The conductive metal sheet, called a thermal doubler, is bonded to an equipment shelf to allow energy to radiate to cooler surroundings from the exposed face and/or to be conducted through the shelf for subsequent radiation to suitable regions. The primary objective of the thermal design is to maintain the temperature of the dissipating component at or below a specified value T (design); an important secondary goal is to minimize the doubler mass.

The thermal design task is intricate because the problem is multiply constrained by all of the following: 1) component power dissipation, Q; 2) maximum allowable component temperature, T (design); 3) component-to-doubler interface area ("footprint"), A_1; 4) maximum available doubler (shelf) area A_3; 5) footprint and doubler (shelf) shape implicit in dimensions ℓ_i and w_i; 6) footprint location within doubler implicit in dimensions Δw and $\Delta\ell$; 7) specified surroundings, $\mathcal{F}_{ij}$, T_j, U_{is}, and T_s; and 8) limited selection of thermal conductivity, k. Frequently, the constraint of simplicity (e.g., manufacturability) is imposed also. The design problem is so highly constrained that seldom is it obvious that any design exists, much less a practical, minimum mass design.

In industrial applications, nodal thermal models using computer codes are commonly used to develop doubler designs. The design proceeds iteratively by specifying a trial doubler thickness and configuration and calculating temperatures; the analytical process is repeated until acceptable temperatures and masses are found. Experience has shown that nodal models are essential to doubler design despite uncertainties introduced by coarse nodal arrangements and the potential expense of making, interpreting, and evaluating numerous computer runs. The analysis and formulation presented here provide an additional analytical tool for doubler designers in the form of an exact solution to a linearized version of the doubler field equation.

A thermal doubler is a two-dimensional fin, but the literature of heat transfer in extended surfaces contains little information on two-dimensional configurations comparable to thermal doublers. References 1-3 contain sections dealing with one-dimensional fins and geometries and boundary conditions associated with pumped fluid or active thermal control systems. References 4-6 are more recent studies of two-dimensional effects in fins, but they are concerned with thick, straight fins and the influence of a wall structure on the performance of a fin. Kraus et al.[7] and Snider and

Received May 20, 1984; presented as Paper 84-1742 at the AIAA 19th Thermophysics Conference, Snowmass, CO, June 25-28, 1984; revision received Nov. 20, 1984.

*Senior Scientist, Space and Communications Group. Associate Fellow AIAA.

†Member of Technical Staff, Space and Communications Group. Member AIAA.

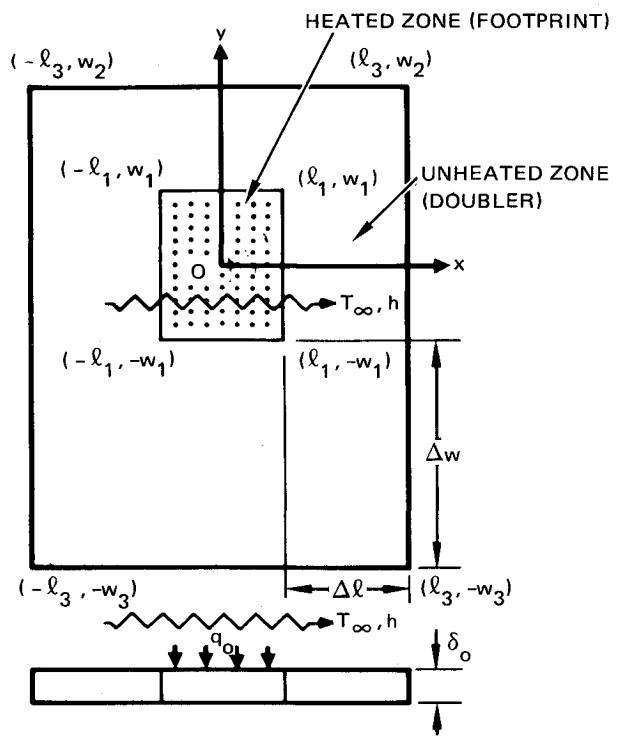

Fig. 1 Schematic of thermal doubler with single symmetry.

Kraus[8] deal with complex geometries inherent in compact heat exchangers, but the analyses are based on one-dimensional fins. Arpaci[9] presents a detailed discussion of a radial, one-dimensional configuration comparable to a thermal doubler in an example dealing with "an empty skillet...forgotten on a hot plate."

The present analysis starts with a two-dimensional, steady-state field equation in Cartesian coordinates and uses the zonal technique of Ref. 9 to develop closed-form solutions. The solution is obtained by linearizing the radiation[3]; the approximation of linearized radiation appears to be reasonable for applications in which the maximum doubler temperature is not significantly higher than the immediate heat sink temperature.

The following section contains a summary of essential analytical details. Following the development of zonal solutions, a doubler design is examined based on typical power levels, dimensions, and environments for a current spacecraft application. The numerical results illustrate the influence of three geometrical parameters on the performance and design of thermal doublers; the geometrical parameters examined below are doubler shape, footprint shape, and footprint location within the doubler boundaries.

Analysis

The geometry of the rectangular thermal doubler of uniform thickness considered here is shown in Fig. 1. The heated footprint occupies the central zone $-\ell_1 \le x \le \ell_1$, $-w_1 \le y \le w_1$; the area available for the doubler occupies the region $-\ell_3 \le x \le \ell_3$, $-w_3 \le y \le w_2$. The doubler and footprint are symmetric about the Y axis. Because of the symmetry about the Y axis, it is necessary to consider the region $0 < x \le \ell_3$, only. A heat load of flux density q_0 is imposed uniformly over the area of the heated footprint, $A_1 = 4w_1\ell_1$. The doubler is assumed to radiate energy from one surface to surrounding surfaces at temperatures $T_1, T_2, \ldots, T_j$ and to conduct energy from the opposite surface to a heat sink at temperature T_s. The thickness of the doubler, δ_0, is substantially less than the dimensions ℓ_1 or w_1 and the thermal conductivity k is assumed to be high so that the temperature difference between the plane doubler surfaces is negligible. Within this framework of assumptions, it may be found[10] that a heat balance on a differential element of volume $\delta_0 dx dy$ at location (x,y) leads to the two-dimensional fin equation

$$k\delta_0\left[\frac{\partial^2 T}{\partial x^2}+\frac{\partial^2 T}{\partial y^2}\right] = \sum_{j=1}^{J} \sigma \mathfrak{F}_j(x,y)\,[T^4 - T_j^4]$$

$$+ U(x,y)\,[T - T_s] - q(x,y) \tag{1}$$

where $U(x,y)$ accounts for conduction through a shelf and convection from the opposite shelf surface.

$$q(x,y) = \begin{cases} q_0, & 0 < x \le \ell_1, \quad -w_1 < y \le w_1 \\ 0, & \begin{cases} \ell_1 < x \le \ell_3, & -w_1 < y \le w_1 \\ 0 < x \le \ell_3 & \begin{cases} w_1 < y \le w_2 \\ -w_3 < y \le -w_1 \end{cases} \end{cases} \end{cases}$$

It is assumed that all of the energy added within the heated footprint is lost from the surfaces and no energy is lost at the boundaries; that is,

$$\frac{\partial T}{\partial x} = 0 \text{ at both } x = 0 \text{ and } \ell_3$$

$$\frac{\partial T}{\partial y} = 0 \text{ at both } y = w_2 \text{ and } -w_3 \tag{2}$$

The numerical solution of the nonlinear field equation is beyond the scope of most engineering design studies. However, the field equation may be reduced to a tractable form if 1) the mean values of $\mathfrak{F}_j(x,y)$ and $U(x,y)$ are used, and 2) the footprint and doubler temperatures are not significantly different from the radiative boundary temperatures. These conditions allow the introduction of a linearized radiation coefficient, h_r, and an equivalent sink temperature, T_∞, defined by the relations

$$h = h_r + \bar{U}, \qquad T_\infty = (h_r T_r + \bar{U} T_s)/h$$

$$T_r^4 = \sum_{j=1}^{J} \bar{\mathfrak{F}}_j T_j^4 \Big/ \sum_{j=1}^{J} \bar{\mathfrak{F}}_j$$

$$h_r = \sum_{j=1}^{J} \sigma \bar{\mathfrak{F}}_j (T_m^2 + T_r^2)(T_m + T_r) \tag{3}$$

where $\bar{\ }$ designates a mean value, r refers to linearized radiation, and T_m is a reference temperature in the range

$$T_\infty < T_m \le T(\max) \tag{4}$$

Using Eqs. (3) and (4) in Eq. (1) leads to a linear field equation

$$k\delta_0\left[\frac{\partial^2 T}{\partial x^2}+\frac{\partial^2 T}{\partial y^2}\right] - h(T - T_\infty) = -q(x,y) \tag{5}$$

This equation is recast in nondimensional form by introducing the following nomenclature:

$$\xi = x/\ell_3, \qquad \eta = y/\ell_3$$

$$\phi(\xi,\eta) = [T(\xi,\eta) - T_\infty]/(q_0\ell_3/k)$$

$$L_i = \ell_i/\ell_3, \qquad W_i = w_i/\ell_3, \qquad Bi = h\ell_3/k$$

$$b^2 = Bi\ell_3/\delta_0, \qquad q(\xi,\eta)/q_0 = f(\xi)g(\eta)$$

$$f(\xi) = \begin{cases} 1, & 0 < \xi \le L_1 \\ 0, & L_1 < \xi \le 1 \end{cases}$$

$$g(\eta) = \begin{cases} 1, & -w_1 < \eta \le w_1 \\ 0, & \begin{cases} w_1 < \eta \le w_2 \\ -w_3 < \eta \le -w_2 \end{cases} \end{cases} \tag{6}$$

It may be observed that Eq. (5) is exact when the doubler operates in a convective environment and the film coefficient h is specified. The boundary value problem is reduced to the expressions

$$\frac{\partial^2\phi}{\partial\xi^2} + \frac{\partial^2\phi}{\partial\eta^2} - b^2\phi = -f(\xi)g(\eta)\ell_3/\delta_0 \tag{7}$$

$$\frac{\partial\phi}{\partial\xi} = 0 \text{ at } \xi = 0,\ 1$$

$$\frac{\partial\phi}{\partial\eta} = 0 \text{ at } \eta = W_2,\ -W_3 \tag{8}$$

Equation (7) may be solved using the separation of variables technique. The piecewise continuous inhomogeneity requires a three-zone solution in η; in the ξ dimension, the inhomogeneity is accommodated by a Fourier series expansion. The zonal solutions are designated as

$$\phi(\xi,\eta) = \phi_1(\xi,\eta) = X(\xi)\,Y(\eta;1), \quad -W_1 < \eta \le W_1$$

$$= \phi_2(\xi,\eta) = X(\xi)\,Y(\eta;2), \quad W_1 < \eta \le W_2$$

$$= \phi_3(\xi,\eta) = X(\xi)\,Y(\eta;3), \quad -W_3 < \eta \le -W_1 \tag{9}$$

Temperature continuity and conservation of energy are invoked at $\eta = \pm W_1$; that is,

$$\phi_1(\xi, W_1) = \phi_2(\xi, W_1)$$

and

$$\left.\frac{\partial\phi_1}{\partial\eta}\right|_{(\xi,W_1)} = \left.\frac{\partial\phi_2}{\partial\eta}\right|_{(\xi,W_1)}$$

$$\phi_1(\xi, -W_1) = \phi_3(\xi, -W_1) \tag{10a}$$

and

$$\left.\frac{\partial\phi_1}{\partial\eta}\right|_{(\xi,-W_1)} = \left.\frac{\partial\phi_3}{\partial\eta}\right|_{(\xi,-W_1)} \tag{10b}$$

After some mathematical manipulations, the solution is found as

$$\phi_i(\xi,\eta) = \frac{1}{Bi}\left\{L_1 Y_0(\eta;i) + \frac{2}{\pi}\sum_{n=1}^{\infty}\left[\frac{\sin n\pi L_1}{n[1+(n\pi/b)^2]}\right][\cos n\pi\xi]\,Y_n(\eta;i)\right\} \tag{11}$$

where

$$Y_n(\eta;1) = 1 - (C_{1n}\cosh\zeta_n\eta + C_{2n}\sinh\zeta_n\eta) \tag{12a}$$

$$Y_n(\eta;2) = C_{3n}\cosh\zeta_n(\eta - W_2) \tag{12b}$$

$$Y_n(\eta;3) = C_{4n}\cosh\zeta_n(\eta + |W_3|) \tag{12c}$$

$$\zeta_n^2 = b^2 + (n\pi)^2 \tag{13}$$

$$C_{1n} = [\sinh\zeta_n(W_2 - W_1)\cosh\zeta_n|W_3| + \sinh\zeta_n(|W_3| - W_1)\cosh\zeta_n W_2]/\sinh\zeta_n(W_2 + |W_3|) \tag{14a}$$

$$C_{2n} = -\sinh\zeta_n(|W_3| - W_2)\sinh\zeta_n W_1/\sinh\zeta_n(W_2 + |W_3|) \tag{14b}$$

$$C_{3n} = 2\sinh\zeta_n W_1\cosh\zeta_n|W_3|/\sinh\zeta_n(W_2 + |W_3|) \tag{14c}$$

$$C_{4n} = 2\sinh\zeta_n W_1\cosh\zeta_n W_1/\sinh\zeta_n(W_2 + |W_3|) \tag{14d}$$

Equations (9) and (11-14) completely define the temperature at any point in the doubler.

Direct and Design Solutions

The temperature field for the doubler may be found by specifying all of the following: q_0, T_∞, h, k, ℓ_1, ℓ_3, w_1, w_2, w_3, and δ_0. Such a solution is termed the direct solution and is useful for examining the influence of the ten parameters on the performance of a doubler assembly. Typically, a thermal designer is most interested in either the maximum or mean temperature of the footprint. Thermodynamic considerations indicate that the maximum will lie on the Y axis within the heated footprint so that only Eqs. (11) and (12a) need be considered. The mean temperature of the footprint may be defined in terms of an integral of Eqs. (11) and (12a).

Usually, the designer must solve for the doubler thickness δ_0 when a maximum allowable temperature is specified. That is, the ten parameters that must be specified are q_0, T_∞, h, k, ℓ_1, ℓ_3, w_1, w_2, w_3, and $T(\max)$. The solution of this inverse or design problem is more difficult because the equation for δ_0 is transcendental and the location of the maximum temperature $(0,\bar{y})$ is unknown. In principle, two transcendental equations must be solved to find doubler thickness, δ_0, based on the maximum temperature, $T(\max) = T(0,\bar{y})$. In practice, it proved to be more efficient to use an iterative procedure to solve for both thickness δ_0 and location $\bar{y}$ corresponding to $T(\max) = T(\text{design})$.

In this study of geometrical effects on the design and performance of thermal doublers, the investigation is limited to a single value of power dissipation; fixed footprint area, A_1; fixed doubler area, A_3; a single set of specified surroundings, $\mathfrak{F}_{ij}$, T_j, U, and T_s; and a single value of thermal conductivity. The geometrical factors examined below are 1) the shape of the heated footprint, 2) the shape of the doubler area, and 3) the location of the footprint along an axis of symmetry. Three parameters are introduced to characterize the geometrical factors:

Footprint shape parameter:

$$\lambda_1 = 2w_1/\ell_1 = 2W_1/L_1 \tag{15a}$$

Doubler shape parameter:

$$\lambda_3 = (w_2 + |w_3|)/\ell_3 = W_2 + |W_3| \tag{15b}$$

Footprint location parameter:

$$\nu = 2(w_2 - w_1)/(w_2 + |w_3| - 2w_1)$$

$$= 2(W_2 - W_1)/(\lambda_3 - \lambda_1 L_1) \tag{15c}$$

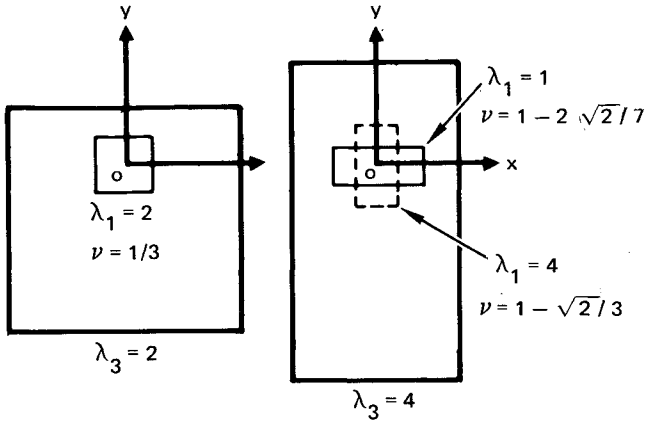

Fig. 2 Plan view of two equal-area doublers with equal-area footprints.

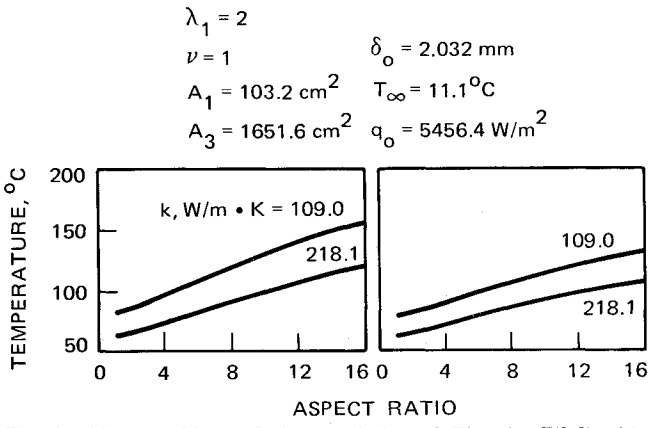

Fig. 3 Direct problem solution: variation of $T(\max) = T(0,0)$ with doubler aspect ratio, $\mathcal{R} = 2/\lambda_3$ (left) true convection, $h = 11.4$ W/m²-K (right) linearized radiation.

Doubler aspect ratio, defined as $\mathcal{R} = 2/\lambda_3$ is convenient for identifying the shape of doubly symmetric doublers. For example, a square footprint corresponds to the case $w_1 = \ell_1$ or $\lambda_1 = 2$; a square doubler corresponds to $w_2 + w_3 = 2\ell_3$ or $\lambda_3 = 2$. Double symmetry occurs if $w_2 = w_3$ or $\nu = 1$; a limiting location of the footprint within the doubler is $w_2 = w_1$ or $\nu = 0$. The shapes and locations of two different doublers and three different footprints are shown in Fig. 2. The manner in which λ_1, λ_3, and ν influence thermal doubler design and performance is demonstrated by considering the following numerical example.

Numerical Example

The following conditions are based on typical thermal doubler requirements for passive temperature control of spacecraft electronic communication components: footprint heat load $Q = 56.304$ W, heated footprint area $A_1 = 103.2$ cm², doubler area $A_3 = 1651.6$ cm², environmental temperature $T_\infty = 11.11°C$, linearized radiation coefficient

$$h_r = 8.535 \times 10^{-8}\ [T^2(\max) + 284.26)^2] \times [T_r(\max) + 284.26]\ W/m^2\text{-K} \quad (16)$$

and doubler thermal conductivity $k = 218.1$ W/m-°C. The study is limited to three values of the footprint shape parameter, $\lambda_1 = 1$, 2, 4, and selected values of the doubler shape parameter in the range $0.125 \le \lambda_3 \le 4$. The location parameter is varied over the range $0 < \nu \le 1$. The dimensions ℓ_1, ℓ_3, w_1, w_2, and w_3 are completely determined by specifying A_1, A_3, λ_1, λ_3, and ν. The direct problem is examined here by considering a doubler of thickness $\delta_0 = 2.032$ mm to determine how the temperature field is influenced by geometry. For the design problem, a maximum allowable temperature, $T(\text{design}) = T(\max) = 62.95°C$, is postulated to show how doubler thickness δ_0 is influenced by geometry.

The linearized radiation coefficient is based, arbitrarily, on the maximum doubler temperature as the reference value [cf. Eq. (4)]. Equation (16) postulates radiation from both upper and lower doubler surfaces to surroundings at a mean temperature of 11.11°C, the mean overall conductance, $\bar{U}$, through an equipment shelf was neglected; that is, in Eq. (3), it was assumed that $\bar{U} = h = h_r$ and $T_s = T_\infty$. For purposes of comparison, some limited results are included for the case of true convection from both sides of the doubler; the "two-sided" value, $h = 11.36$ W/m²-°C, was chosen to provide insight into the case of heat loss from both sides of A_3 including A_1 by natural convection to a fluid with a bulk temperature of 11.11°C. It may be observed that the temperature $T(\max)$ is unknown when solving the direct problem based on linearized radiation; an iterative process was used to solve for $T(\max)$ and h_r simultaneously. Calculations for true convection neglect radiation, while those for linearized radiation omit convection.

Results

Equations (9) and (11-14) were coded for an IBM 3081 computer. Several analytical experiments were conducted to verify the code and identify the program operating characteristics. It was found that only 15 terms of the infinite series were required to calculate temperatures that were precise to eight decimal places at all locations in the doubler field. The code was verified by comparing the infinite series solution to the simple one-dimensional case that follows by letting $L_1 = 1$ and $w_2 = w_3$. A second bound was sought by comparing the infinite series direct solution for a doubly symmetric square footprint/square doubler ($\lambda_1 = \lambda_3 = 2$, $\nu = 1$) to the one-dimensional, axisymmetric, direct case of a circular footprint/circular doubler (see Appendix) operating with identical heat loads, areas, and environmental conditions. It was found, unexpectedly, that the maximum temperatures for the square and circular geometries were virtually identical.

Results for the direct problem are shown in Figs. 3-6. Figures 3 and 4 apply for a doubly symmetric configuration for which the heated footprint was maintained as a square ($\lambda_1 = 2$) and the doubler shape was varied from a square ($\lambda_3 = 2$ or $\mathcal{R} = 1$) to a long narrow rectangle ($\lambda_3 = 0.125$ or $\mathcal{R} = 16$). The results for $\mathcal{R} = 16$ may be obtained from the solution for a one-dimensional doubler. Figure 3 shows how the maximum temperature increases in a near linear manner as the aspect ratio increases. A comparison of Figs. 3a and 3b shows that the change in $T(\max)$ is less pronounced for the case of linearized radiation than for true convection. Results are shown for two values of thermal conductivity which approximate the range of conductivities available in wrought aluminum alloys.

Isotherm plots based on true convection are shown in Figs. 4 and 5 for several configurations. Comparable trends appeared for linearized radiation plots, but the temperature spread was smaller and the isotherms were farther apart. Figure 4a shows isotherms for both square/square and circular/circular doublers of equal areas, heat loads, environmental conditions, and thickness. The maximum temperatures were 62.99 and 62.96°C for the circle and the square, respectively. The similarity of the two maxima and the isotherm patterns suggests that the simple formulation for a circular doubler serves as a good approximation for a square doubler. All of the configurations of Fig. 4 are doubly symmetric with a square footprint ($\lambda_1 = 2$). In Fig. 5a the doubler is also doubly symmetric, but the heated footprint is a 2:1 rectangle ($\lambda_1 = 4$). It may be observed that the doubler shape ($\lambda_3 = 1$) in Fig. 4b is identical to the doubler

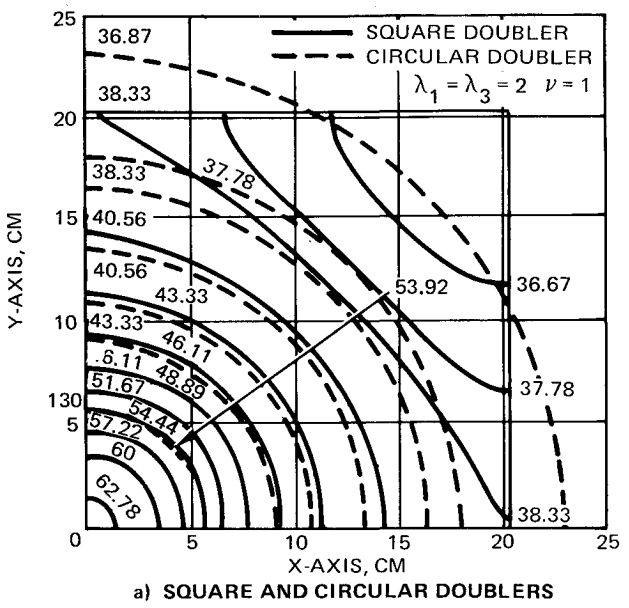

a) SQUARE AND CIRCULAR DOUBLERS

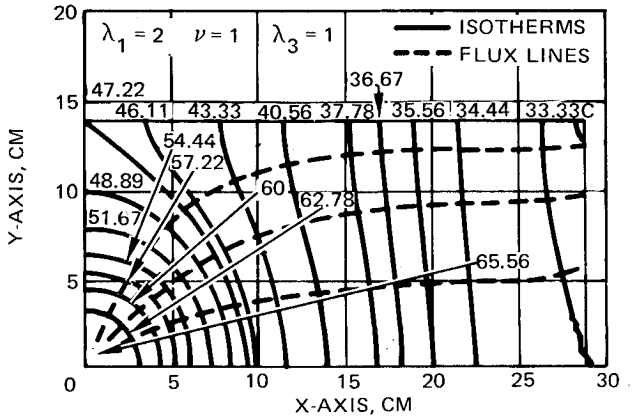

b) ISOTHERMS AND FLUX LINES ON 2:1 RECTANGULAR DOUBLER

Fig. 4 Isotherm maps.

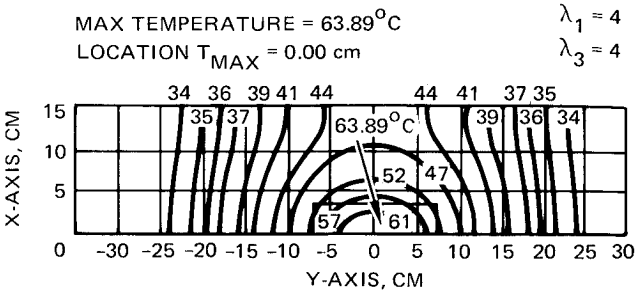

a) FOOTPRINT LOCATION AT $\nu = 1$

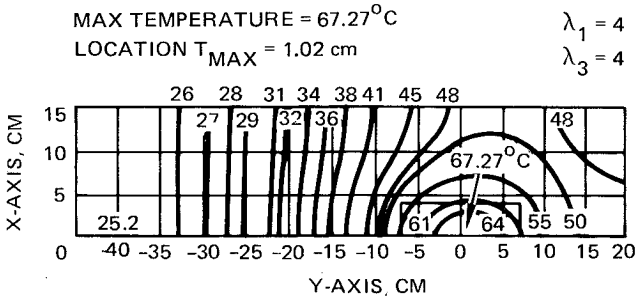

b) FOOTPRINT LOCATION AT $\nu = 0.5$

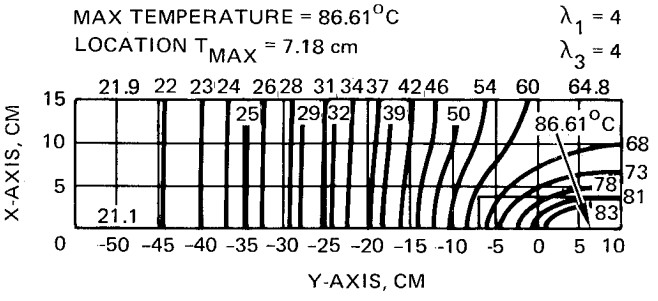

c) FOOTPRINT LOCATION AT $\nu = 0$

Fig. 5 Isotherm maps.

shape in Fig. 5a ($\lambda_3 = 4$) insofar as the ℓ_3 and w_2 dimensions are interchangeable. The areas and conditions for Fig. 5 are the same as in Fig. 3a. Note the change in the X and Y axes in Fig. 5. In Fig. 5c, the condition has single symmetry for $A_1 = 103.2$ cm^2 and $A_3 = 1651.6$ cm^2, and double symmetry for $A_1 = 206.5$ cm^2 and $A_3 = 3303.2$ cm^2.

Figure 6 shows the magnitude and location of the maximum temperature for six combinations of λ_1 and λ_3. Figure 6 was developed for linearized radiation; similar trends were found for true convection but higher maxima occur for $\nu < 1$. Table 1 contains a summary of maximum temperatures for both linearized radiation and true convection.

Results for the design case are presented in Figs. 7 and 8 and in Table 2. Figure 7 was developed for the same doubly symmetric configuration examined in the direct problem; i.e., square footprint ($\lambda_1 = 2$) and $1 < \mathcal{R} \leq 16$ ($2 > \lambda_3 \geq 0.125$). The thickness δ_0 is seen to increase with aspect ratio in a near linear manner. Once again, the two curves in Fig. 7 approximate the range of thermal conductivity values available for wrought aluminum; it is significant that doubler thickness varies inversely as thermal conductivity.

Figure 8 shows how thickness and location of $T(\max) = T(\text{design})$ vary with footprint location for six combinations of λ_1 and λ_3. It is seen that doubler thickness is least for doubly symmetric geometries ($\nu = 1$) and thickness increases 12-18% as the footprint location is changed to $\nu = 0.5$; the increase in thickness is very marked as ν approaches zero. The shift of the location of $T(\max)$ appears to be influenced more by the footprint location ν than by the shape parameters λ_1 and λ_3.

Discussion

The closed-form solution given by Eqs. (11-14) is quite simple and the equations can be programmed for any of several different personal computers. Indeed, if maximum temperature and/or doubler thickness are the only variables of interest, a useful doubler code can be limited to Eqs. (11), (12a), (13), (14a), and (14b). With such a code, a thermal analyst/designer would be able to make rapid estimates of doubler performance and mass with accuracy suitable for most preliminary design applications.

The numerical results presented here are not intended to be a catalog for doubler designers. Instead, the numerical results are intended 1) to show the type of results that may be developed from the closed-form equations, 2) to gain insight into analytical relations and geometrical influences, and 3) to serve as a standard of comparison for numerical solutions based on finite difference or finite element models. The numerical results illustrate the nature of trade studies that may be made to define a preliminary design for a doubler application. In other design situations a designer could investigate the influence of other parameters such as the sink temperature, T_∞; overall conduction coefficient, U; radiation coupling factors, $\mathcal{F}_{ij}$; etc. Following the definition of a preliminary design, it would be necessary to develop a nodal model to account for T^4 radiation and nonuniformities that cannot be accommodated by the closed-form solution.

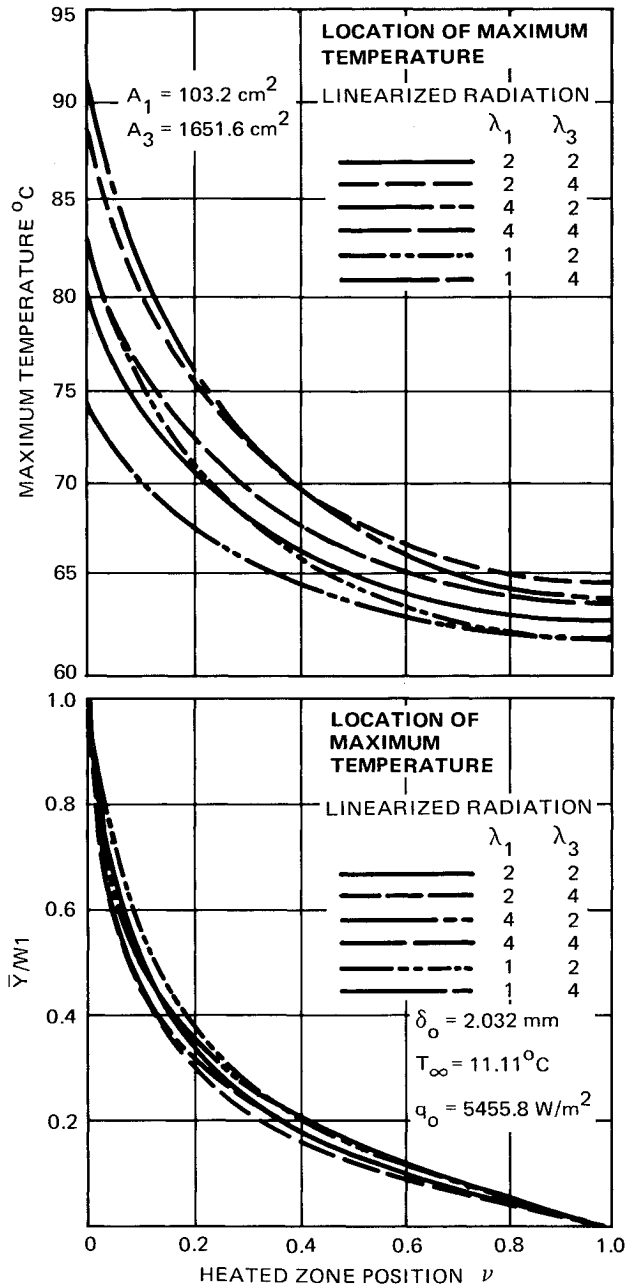

Fig. 6 Magnitude and location of maximum temperature for six different doubler geometries.

An important insight found in the present study is the relationship between radial and Cartesian one-dimensional solutions. Equations (A7) and (A10) in the Appendix are simple expressions that may be coded for programmable hand calculators. These equations may be used to solve for thicknesses, δ_0 (radial) and δ_0 (Cartesian); the results developed here indicate that the thickness of a circular doubler is virtually identical to the thickness of a square/square ($\lambda_1 = \lambda_3 = 2$, $\nu = 1$) doubler of equal area and heat load, etc. The near linear variation of thickness with aspect ratio (Fig. 7) suggests that the thickness of a doubly symmetric doubler may be estimated by interpolation between the radial and Cartesian one-dimensional limits.

Finally, the closed-form solution may be used as a standard for evaluating the accuracy of a nodal model. The closed-form solution is both an approximate solution to a design problem and an exact solution to a boundary value problem. Numerical solutions based on nodal models also

Table 1 Comparison of maximum temperature for true convection $h = 11.36$ W/m^2-°C and linearized radiation ($\delta_0 = 2.032$ mm)

ν	λ_1	λ_3	True convection, T(max), °C	Linearized radiation, T(max), °C
0	1	2	85.41	81.98
		4	96.86	90.80
	2	2	82.82	79.79
		4	93.71	88.26
	4	2	76.41	74.38
		4	86.61	82.47
0.5	1	2	65.24	64.92
		4	68.84	67.94
	2	2	65.89	65.48
		4	69.32	68.35
	4	2	64.04	63.89
		4	67.27	66.62
1.0	1	2	61.75	61.92
		4	64.29	64.10
	2	2	62.96	62.96
		4	65.29	64.96
	4	2	61.76	61.92
		4	63.89	63.76

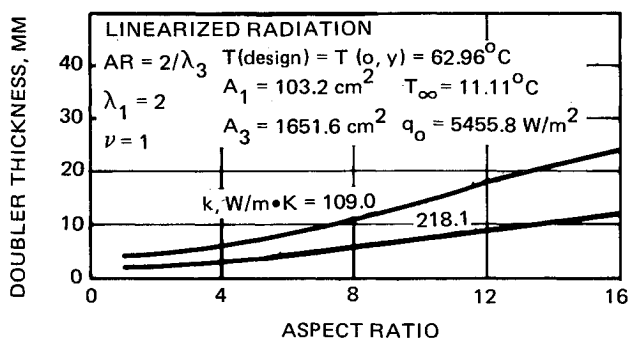

Fig. 7 Design problem solution: variation of doubler thickness with doubler aspect ratio—linearized radiation.

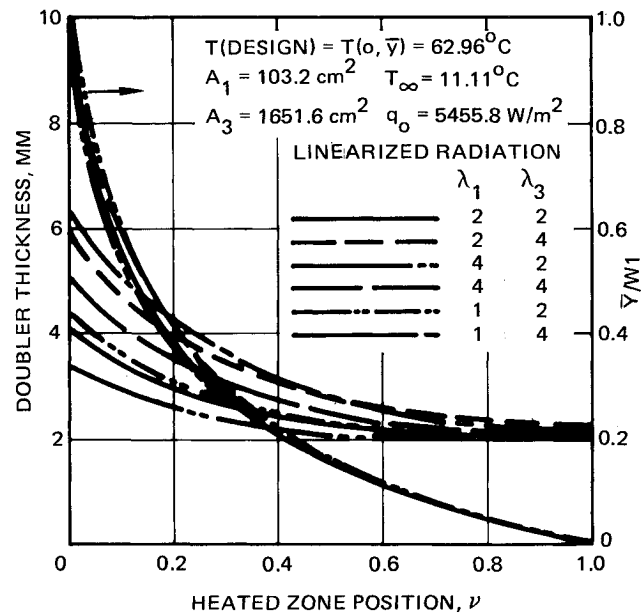

Fig. 8 Design problem solution: thickness and location of T(max)—linearized radiation.

Table 2 Summary of geometrical influence on doubler thickness $T(\text{design}) = T(\text{max}) = 62.96°C$

ν	λ_1	λ_3	δ_0, mm
0	1	2	4.50
		4	6.50
	2	2	4.22
		4	6.10
	4	2	3.51
		4	5.18
0.5	1	2	2.26
		4	2.72
	2	2	2.31
		4	2.77
	4	2	2.13
		4	2.51
1.0	1	2	1.91
		4	2.16
	2	2	2.03
		4	2.26
	4	2	1.91
		4	2.11

provide an approximate solution to a design problem but at a different level of approximation. The closed-form solution given here may be used as a basis for calibrating or adjusting a nodal model of a doubler by modifying nodal model inputs to accommodate linearized radiation and an equivalent sink temperature. This implies the expectation that "production calculations" will have comparable accuracy when T^4 radiation and various sink temperatures are restored.

Summary and Conclusions

A closed-form solution has been developed for a two-dimensional, thin, extended surface with configuration and boundary conditions comparable to a thermal doubler. The geometry consists of a rectangular footprint within a larger rectangular heat-loss zone. An exact solution is presented for a steady-state, two-dimensional, partial differential equation with a piecewise continuous inhomogeneity. For the range of parameters investigated, the first through fifteenth terms of an infinite series provided precision to eight decimal places.

A numerical problem was examined using a heat load, dimensions, and environmental conditions typical of a communications satellite application. During the course of a numerical study, it was found that the solution for a doubly symmetric square footprint/square doubler yielded virtually the same maximum temperature as an axisymmetric circular footprint/circular doubler of equal thickness, heat load, and area; furthermore, it was observed that solutions for one-dimensional radial and Cartesian doublers provide lower and upper bounds for the maximum temperature or thickness of a double symmetric rectangular doubler with a square footprint and width/height ratio greater than 1.

The range of parameters examined here was too limited to develop a catalog of design characteristics; however, for the range of parameters it was found that maximum temperature or doubler thickness depends on the parameters in the following order of importance: 1) footprint location, 2) doubler shape, 3) footprint shape. The thinnest doubler (i.e., lowest mass) occurs for the case of double symmetry for a 2:1 footprint in a square doubler.

The closed-form solution is quite simple and the single symmetry, two-dimensional equations may be coded for any of several personal computers. It is believed that the closed-form solution will be useful for making trade studies required to define a preliminary design; however, doubler design details required for a final design should be developed using a finite difference or finite element nodal model. The closed-form solution may be used as a reference to calibrate or adjust a nodal model.

Appendix: One-Dimensional Doublers

The geometry of a circular doubler of thickness δ_0 consists of a heated footprint of radius r_1 centered on a larger unheated area of radius r_3. The field equation for this doubler may be expressed as

$$\frac{1}{\rho}\frac{\mathrm{d}}{\mathrm{d}\rho}\left(\rho\frac{\mathrm{d}\phi}{\mathrm{d}\rho}\right) - \tilde{b}^2\phi = -\frac{r_3}{\delta_0}f(\rho) \tag{A1}$$

where

$$\rho = \frac{r}{r_3}, \quad \phi(\rho) = \frac{[T(\rho) - T_\infty]}{(q_0 r_3/k)}$$

$$\tilde{Bi} = hr_3/k, \quad \tilde{b}^2 = \tilde{Bi}r_3/\delta_0, \quad R_1 = r_1/r_3$$

$$f(\rho) = 1, \quad 0 < \rho \le R_1$$

$$= 0, \quad R_1 < \rho \le 1 \tag{A2}$$

The boundary conditions are

$$\partial\phi/\partial\rho = 0 \text{ at } \rho = 0, 1 \tag{A3}$$

A zonal solution is developed such that $\phi(\rho) = \phi_1(\rho)$, $0 < \rho \le R_1$, and $\phi(\rho) = \phi_2(\rho)$, $R_1 < \rho \le 1$ with matching conditions at $\rho = \mathrm{R}_1$:

$$\phi_1(R_1) = \phi_2(R_1) \quad \text{and} \quad \phi_1'(R_1) = \phi_2'(R_1) \tag{A4}$$

The solution for the circular doubler may be expressed as

$$\phi_1(\rho) = \frac{1}{\tilde{Bi}}[1 - C_1 I_0(\tilde{b}\rho)], \quad 0 < \rho \le R_1$$

$$\phi_2(\rho) = \frac{C_2}{\tilde{Bi}}[K_1(\tilde{b})I_0(\tilde{b}\rho) + I_1(\tilde{b})K_0(\tilde{b}\rho)], \quad R_1 < \rho \le 1 \tag{A5}$$

$$C_1 = (\tilde{b}R_1)[I_1(\tilde{b})K_1(\tilde{b}R_1) - K_1(\tilde{b})K_0(\tilde{b}\rho)]/I_1(\tilde{b})$$

$$C_2 = (\tilde{b}R_1)I_1(\tilde{b}R_1)/I_1(\tilde{b}) \tag{A6}$$

where $I_p(z)$ and $K_p(z)$ are modified Bessel functions of the first and second kind of order p, respectively. The maximum temperature occurs at $\rho = 0$ and has the magnitude

$$\phi(\max) = \phi_1(0) = \frac{1}{\tilde{Bi}}(1 - C_1) \tag{A7}$$

A Cartesian one-dimensional solution may be obtained by setting $L_1 = 1$ in Eq. (11) to find

$$\phi_1(\eta) = \frac{1}{Bi}[1 - C_{1,0}\cosh b\eta - C_{2,0}\sinh b\eta], \quad -W_1 < \eta \le W_1 \tag{A8}$$

where $C_{1,0}$ and $C_{2,0}$ are given by Eqs. (14a) and (14b). The location and magnitude of the maximum temperature are easily found by setting the derivative of $\phi_1(\eta)$ equal to zero with the result

$$\phi(\max) = \phi_1(\bar{\eta}) = \frac{1}{Bi}[1 - \sqrt{C_{1,0}^2 - C_{2,0}^2}] \tag{A9}$$

Equation (A9) represents the design formula for a Cartesian one-dimensional doubler. For the doubly symmetric case,

$w_2 = w_3$, the design formula reduces to

$$\phi(\max) = \phi_1(0) = \frac{1}{Bi}[1 - C_{1,0}] \qquad \text{(A10)}$$

Acknowledgment

The authors gratefully acknowledge the role of Jerry Lewis, Hughes Aircraft Company, Space and Communications Group, who identified the problem of thermal doubler design and suggested the need for an exact solution.

References

[1]Sparrow, E. M. and Cess, R. D., *Radiation Heat Transfer*, Augmented Edition, Hemisphere Publishing Corp., 1978, pp. 180-189.

[2]Siegel, R. and Howell, J. R., *Thermal Radiation Heat Transfer*, 2nd Ed., Hemisphere Publishing Corp., 1981, pp. 384-396.

[3]Edwards, D. K., *Radiation Heat Transfer Notes*, Hemisphere Publishing Corp., 1981, pp. 329-362.

[4]Heggs, P. J. and Stones, P. R., "The Effects of Dimensions on the Heat Flowrate through Extended Surfaces," *ASME Journal of Heat Transfer*, Vol. 102, No. 1, Feb. 1980, pp. 180-182.

[5]Heggs, P. J., Ingham, D. B., and Manzoor, M., "The Analysis of Fin Assembly Heat Transfer by a Series Truncation Method," *ASME Journal of Heat Transfer*, Vol. 104, No. 1, Feb. 1982, pp. 210-212.

[6]Suryanarayana, N. V., "Two-Dimensional Effects on Heat Transfer Rates from an Array of Straight Fins," *ASME Journal of Heat Transfer*, Vol. 99, No. 1, Feb. 1977, pp. 129-132.

[7]Kraus, A. D., Snider, A. D., and Doty, L. F., "An Efficient Algorithm for Evaluating Arrays of Extended Surface," *ASME Journal of Heat Transfer*, Vol. 100, No. 2, May 1978, pp. 288-293.

[8]Snider, A. D. and Kraus, A. D., "A General Extended Surface Analysis Method," *ASME Journal of Heat Transfer*, Vol. 103, No. 4, Nov. 1981, pp. 699-704.

[9]Arpaci, V. S., *Conduction Heat Transfer*, Addison-Wesley Publishing Co., Redding, MA, 1966, pp. 151-155.

[10]Carslaw, H. S. and Jaeger, J. C., *Conduction of Heat in Solids*, 2nd Ed., 1959, p. 169.